Frictional properties and sliding stability of the San Andreas fault from deep drill core

B.M. Carpenter, D.M. Saffer, and C. Marone
Department of Geosciences and Energy Institute Center for Geomechanics, Geofluids, and Geohazards, The Pennsylvania State University, University Park, Pennsylvania 16802, USA

ABSTRACT

The strength of tectonic faults and the processes that control earthquake rupture remain central questions in fault mechanics and earthquake science. We report on the frictional strength and constitutive properties of intact samples across the main creeping strand of the San Andreas fault (SAF; California, United States) recovered by deep drilling. We find that the fault is extremely weak (friction coefficient, μ = ~ 0.10), and exhibits both velocity strengthening frictional behavior and anomalously low rates of frictional healing, consistent with aseismic creep. In contrast, wall rock to the northeast shows velocity weakening frictional behavior and positive healing rates, consistent with observed repeating earthquakes on nearby fault strands. We also document a sharp increase in strength to values of μ > ~0.40 over <1 m distance at the boundary between the fault and adjacent wall rock. The friction values for the SAF are sufficiently low to explain its apparent weakness as inferred from heat flow and stress orientation data. Our results may also indicate that the shear strength of the SAF should remain approximately constant at ~10 MPa in the upper 5–8 km, rather than increasing linearly with depth, as is commonly assumed. Taken together, our data explain why the main strand of the SAF in central California is weak, extremely localized, and exhibits aseismic creep, while nearby fault strands host repeating earthquakes.

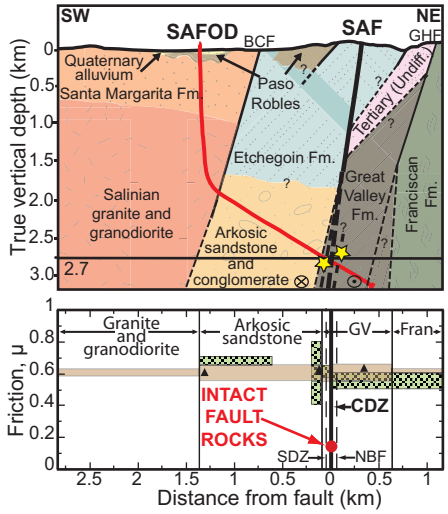

Figure 1. Upper panel: cross section showing key lithologies, fault strands, and San Andreas Fault Observatory at Depth (SAFOD) borehole (Thayer and Arrowsmith, 2005; Zoback et al., 2011). Horizontal line at 2.7 km indicates depth at which borehole intersected two main strands of San Andreas fault (SAF). Stars indicate approximate position of repeating earthquake clusters. BCF—Buzzard Canyon fault; GHF—Gold Hills fault; Undiff.—Undifferentiated; Fm.—Formation. Lower panel: Coefficient of sliding friction versus distance from SAF, showing previously published data from outcrop samples (tan boxes) and SAFOD Phase I borehole cuttings (Carpenter et al., 2009) (black triangles), and borehole cuttings from Phases I and II (green boxes; Tembe et al., 2006). Large red circle shows mean value of intact fault rock from Phase III drilling (this study). Dashed lines define damage zone for SAF bounded by southwest deforming zone (SDZ) and northeast bounding fault (NBF). CDZ—central deforming zone; GV—Great Valley; Fran—Franciscan.

INTRODUCTION

Understanding processes that control the strength and style of slip along Earth's plate boundary fault systems is a long-standing and fundamental problem in the earth sciences. The San Andreas fault (SAF) in California (United States) has been a focal point for research on earthquake physics and the nature of major faults that bound Earth's tectonic plates. Major recent fault-zone drilling initiatives, including the San Andreas Fault Observatory at Depth (SAFOD) (Zoback et al., 2011), the Taiwan-Chelungpu (Ma et al., 2006) drilling project, and the Nankai Trough Seismogenic Zone Experiment (NanTroSEIZE) (Kinoshita et al., 2009), have aimed to penetrate and sample major tectonic faults to characterize the conditions and rock properties that govern their mechanical behavior. In the summer of 2007, the SAFOD borehole (Fig. 1) crossed a creeping segment of the SAF and recovered the first intact samples of the fault zone from seismogenic depths, allowing detailed investigation of the frictional behavior of material spanning the active fault.

Along the SAF, fault weakness has been inferred from both the lack of a prominent thermal anomaly centered over the fault trace (the "heat flow paradox"; e.g., Lachenbruch and Sass, 1980) and the high angle between the maximum horizontal principal stress and the fault trace (Zoback et al., 1987; Hickman and Zoback, 2004). These data indicate that the SAF is weak (1) in an absolute sense, meaning that it supports shear stresses of <20 MPa averaged over the seismogenic crust, substantially lower than predicted by typical laboratory measurements of rock friction; and (2) in a relative sense, meaning that it is considerably weaker than the surrounding crust. A wide range of hypotheses to explain these observations has been proposed. These include locally elevated pore fluid pressure within the fault zone that reduces the effective normal stress (Rice, 1992; Fulton and Saffer, 2009), low friction owing to a combination of intrinsically weak minerals, shear-induced fabric, or nanocoatings on slip surfaces (e.g., Collettini et al., 2009; Schleicher et al., 2010), stress relaxation by pressure solution creep (Gratier et al., 2011), or a combination of these mechanisms (Holdsworth et al., 2011). Dynamic weakening mechanisms such as thermal or acoustic weakening, melting, or silica gel lubrication may also operate, but only along portions of the fault that fail in seismic slip (e.g., Melosh, 1996; Goldsby and Tullis, 2002; Di Toro et al., 2011).

Despite extensive study, the causes of mechanical weakness of tectonic faults and the underlying controls on observed slip behaviors that range from aseismic creep to failure in repeating earthquakes remain elusive. Studies performed on outcrop samples and material from the SAFOD project have provided a regional picture of friction across the SAF and show that the crust surrounding the fault is strong (μ > ~0.5), whereas the fault zone is weaker (μ < ~0.3) (Tembe et al., 2006; Carpenter et al., 2009, 2011; Lockner et al., 2011) (Fig. 1). Initial work on fault rocks recovered from SAFOD has focused primarily on overall frictional strength, and has reported friction data only from drilling cuttings, powdered fault gouge, and rock fragments. These samples lack intact fabric and thus may behave differently than in situ fault rock (e.g., Collettini et al., 2009; Schleicher et al., 2010; Holdsworth et al., 2011). Here we report on friction measurements for a suite of intact and powdered core samples obtained from SAFOD drilling across the main creeping strand of the SAF. Our data address (1) the friction constitutive properties, including the velocity dependence of friction and healing, that dictate fault sliding stability and earthquake physics; and (2) the detailed spatial distribution of frictional properties across the main active fault strand.

GEOLOGY, August 2012; v. 40; no. 8; p. 759–762; doi:10.1130/G33007.1; 4 figures; Data Repository item 2012207. | Published online 15 June 2012.

MATERIALS AND METHODS

Samples collected during SAFOD Phase III include intact core and drill cuttings spanning the main, actively creeping SAF strand, termed the central deforming zone (CDZ) (Fig. 1) (Zoback et al., 2011). Repeated casing deformation logs document that the CDZ, a 2.6-m-wide zone of highly sheared fault gouge, accommodates significant right-lateral motion by aseismic creep (Fig. DR1 in the GSA Data Repository[1]) (Zoback et al., 2011). SAFOD drilling intersected 2 additional important fault strands: (1) a 1.5-m-wide fault zone 108 m southwest of the CDZ, termed the southwest deforming zone (SDZ); and (2) a fault 111 m to the northeast, termed the northeast bounding fault (NBF) (Zoback et al., 2011). The SDZ and NBF mark the interpreted boundaries of an ~200-m-wide damage zone that contains the CDZ. Precise locations of three repeating microearthquake clusters (M_w ~2.0) in the vicinity of the SAFOD borehole show that they occur on the SDZ and NBF (Fig. 1; Thurber et al., 2010). The HI (Hawaii) earthquake cluster occurs on the SDZ ~100 m downdip of the SAFOD borehole penetration of this fault strand, and the SF (San Francisco) and LA (Los Angeles) clusters are interpreted to occur on the updip extension of the NBF (Thurber et al., 2010).

We conducted our experiments on a suite of samples obtained from SAFOD Phase III core, including one sample from wall rock southwest of the CDZ, five from the CDZ, and one from wall rock to the northeast (Figs. 1 and 2). All of the wall-rock samples are from within the 200-m-wide damage zone surrounding the CDZ. X-ray diffraction (XRD) shows that the samples are composed dominantly of clays and quartz (Fig. DR2). Both XRD and thin-section analyses indicate that the CDZ contains significant saponite (as much as ~60 wt%), a Mg-bearing smectite clay (Lockner et al., 2011). Visual and SEM analyses show that pervasive thin shear zones within the CDZ may locally contain as much as 100% saponite. The wall-rock samples on either side of the CDZ are composed dominantly of quartz, calcite, and feldspar, with trace amounts of chlorite in the wall rock to the southwest, and minor lizardite in wall rock to the northeast.

We sheared samples at effective normal stresses ranging from 7 to 100 MPa under controlled pore pressures ranging from 3 to 20 MPa, using a synthetic brine designed to match the major ion chemistry of fluids observed in the SAFOD borehole (Thordsen et al., 2005). Our experiments focused on intact wafers of fault material (4.2 cm × 4.0 cm × ~0.6 cm), augmented with tests using powdered gouge. The wafers were carefully cut from intact core to ensure shearing parallel to the in situ fault shear direction and fault zone fabric, placed in the single-direct-shear configuration (Fig. DR3), jacketed, and sheared in a triaxial pressure vessel. In this configuration, one side of the sample assembly is coated with molybdenum grease, which provides a nearly frictionless contact between the mirror-finished surfaces of the sample assembly and sliding block (equivalent μ = 0.001 for normal stresses 0–100 MPa). For experiments on powdered gouge, samples were pulverized and sieved to <150 μm, and sheared in a double-direct shear geometry (for detailed description of this configuration, see Ikari et al., 2009).

Samples were saturated overnight at an effective normal stress of ~5 MPa, and then loaded to the target normal stress and allowed to equilibrate until sample thickness reached a steady state. Samples were then sheared at a load point velocity of 10 μm/s until a steady-state value of friction was obtained. We measured frictional strength (defined as the ratio of shear stress to effective normal stress and assuming no cohesion), and then conducted velocity stepping and slide-hold-slide tests to measure the friction constitutive properties (e.g., Marone, 1998) (Fig. 2). We conducted velocity steps in the range of 1–100 μm/s, and holds ranging from 3 to 1000 s.

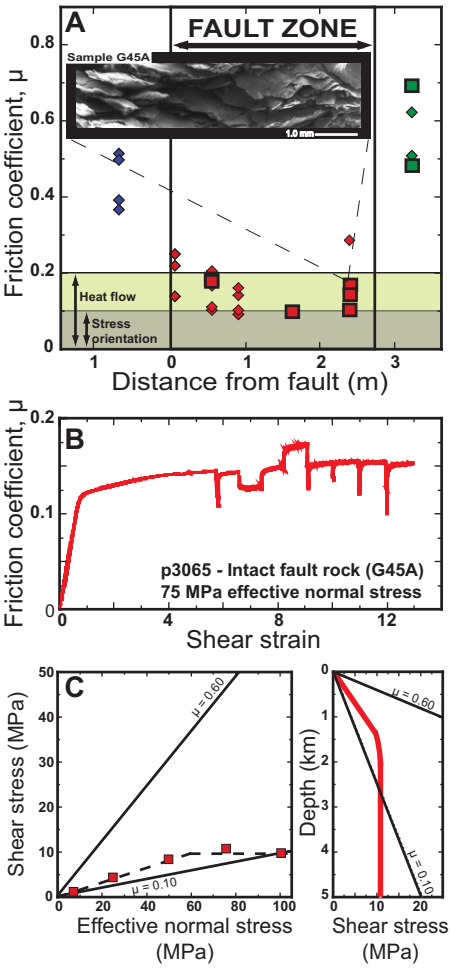

Figure 2. A: Coefficient of sliding friction for samples recovered from San Andreas Fault Observatory at Depth (SAFOD) Phase III coring, as function of distance from southwest edge of central deforming zone (CDZ) mapped in cores (Zoback et al., 2011). Data are shown for shearing of intact wafers (squares) and powdered gouge (diamonds). Limits on effective friction coefficient from heat flow measurements (Lachenbruch and Sass, 1980) and directional constraints (Zoback et al., 1987) for the San Andreas fault (SAF) in central California are shown for reference. Directional constraint determined locally from SAFOD pilot hole stress data at 2.2 km depth is μ = 0.09–0.41 (Hickman and Zoback, 2004). Inset: Scanning electron microscope image of sample G45A from CDZ, showing well-developed shear fabric. B: Example of experimental data showing friction coefficient versus shear strain. C: Mohr-Coulomb failure envelope for wafers of intact fault rock from CDZ. Our data document transition to pressure-independent shear strength at ~60 MPa effective normal stress (left). Corresponding shear strength as function of depth is shown at right, assuming linear increase in fault-normal stress of 50.5 MPa/km (after Hickman and Zoback, 2004), and hydrostatic pore fluid pressure.

Our results show that material from the CDZ is extraordinarily weak (μ = 0.09–0.25), with the lowest friction values in the center of the fault

FRICTIONAL STRENGTH OF THE MAIN SAN ANDREAS FAULT STRAND AND WALL ROCK

[1]GSA Data Repository item 2012207, supplemental and supporting data, is available online at www.geosociety.org/pubs/ft2012.htm, or on request from editing@geosociety.org or Documents Secretary, GSA, P.O. Box 9140, Boulder, CO 80301, USA.

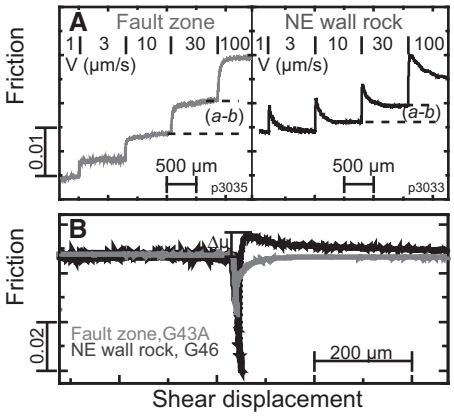

Figure 3. A: Velocity (V) step data from two representative experiments. The friction rate parameter (*a-b*) is measured for each velocity step as shown. B: Data showing friction as function of shear displacement for samples from central deforming zone (CDZ; gray) and wall rock from northeast (black), with 30 s hold shown at center of image; Δμ (μ—friction coefficient) is measured for each hold as shown.

(Fig. 2). We also document a sharp transition to substantially stronger wall rock to both the northeast and southwest (μ > 0.4) over a distance of <1 m (Fig. 2A). Our data are consistent with previously reported friction values for outcrop samples (Carpenter et al., 2009), cuttings (Tembe et al., 2006; Carpenter et al., 2009), and powdered and remolded SAFOD core material (Lockner et al., 2011), and confirm that the SAF at these depths is an intrinsically weak fault embedded in a stronger crust. The friction values we report are sufficiently low to explain both the absolute and relative weakness of the SAF as inferred from heat flow and stress orientation constraints (Fig. 2A).

At effective normal stresses <60 MPa (corresponding to depths <~1.5 km) the friction coefficients we measured for both the CDZ and wall rock are similar for intact fault wafers and powdered gouge (Fig. 2A). However, intact wafers from the CDZ appear to exhibit pressure-insensitive shear strength at higher effective normal stresses (Fig. 2C), whereas powdered gouge does not. This is consistent with previous work showing that fabric defined by clay alignment and thin phyllosilicate grain coatings may result in fault weakening (Collettini et al., 2009; Schleicher et al., 2010; Holdsworth et al., 2011); this fabric is preserved in our intact wafers but not in powdered gouge. This result is also consistent with a transition to pressure-independent strength (i.e., plastic yielding) at normal stresses >30–40 MPa observed in synthetic clay-rich fault gouges, interpreted to reflect saturation of the area of real frictional contact between platy phyllosilicate grains (Saffer and Marone, 2003). Our data imply that the shear strength of the main SAF strand may remain ~10 MPa throughout the depth range where Mg-smectite clay phases remain stable (Inoue and Utada, 1991), rather than increasing linearly with depth, as is commonly assumed (Fig. 2C). Based on the geochemical and thermal environment at SAFOD, saponite is likely to remain stable as a distinct phase and in chlorite-smectite interlayers to depths of 5–8 km; at higher temperatures it transforms to corrensite, but can remain stable in mixed-layer clays to temperatures of >200 °C (~7–8 km depth) (Inoue and Utada, 1991). At greater depths, if the fault zone protolith remains the same as observed at SAFOD, we anticipate that chlorite would be the dominant clay phase and would remain thermodynamically stable to the base of the seismogenic zone (see the discussion in Holdsworth et al., 2011).

FRICTIONAL STABILITY AND HEALING

Both intact wafers and powdered gouge from the CDZ and wall rock to the southwest exhibit exclusively velocity strengthening frictional behavior, with values of (*a-b*) ranging from 0.004 to 0.019 for material from the CDZ, and 0.004 to 0.023 for the wall rock (Fig. 4A). For wall rock to the northeast of the CDZ, we observe instances of velocity weakening behavior only in intact wafers [(*a-b*) = –0.003–0.006], and only velocity strengthening behavior for powdered gouge [(*a-b*) = 0.001–0.006] (Fig. 4A). All of the wall-rock samples we tested exhibit typical frictional behavior, with an immediate increase in friction (the so-called direct effect) followed by displacement-dependent weakening (state evolution). In contrast, samples from the CDZ show no state evolution (Fig. 3A). We also find

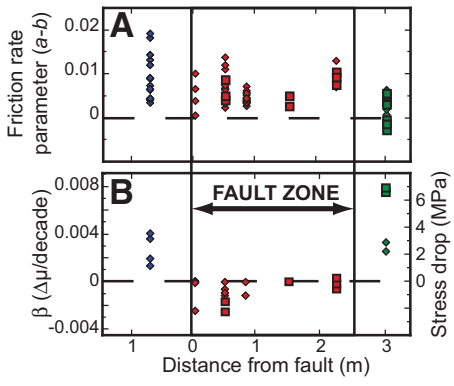

Figure 4. A: Friction rate parameter (*a-b*) as a function of distance from edge of central deforming zone (CDZ). (B) Rate of frictional restrengthening (β) (μ—friction coefficient) measured during slide-hold-slide tests. Diamonds—powdered gouge; squares—intact wafers. Corresponding stress drops shown in B are computed from measured healing rates (Fig. DR4 [see footnote 1]), assuming 1000 d recurrence interval (Nadeau et al., 2004) and effective normal stress of 110 MPa.

that material from the CDZ exhibits no frictional healing (Fig. 3B), whereas the adjacent wall rock exhibits positive healing rates, with the highest values for wall rock to the northeast of the CDZ (Fig. 4B). Together, these results demonstrate a type of frictional behavior that may be significant in tectonic faults, in which the static yield strength is as low as or lower than the dynamic frictional strength. One key implication is that seismic stress drop would be zero or negative. The extremely low healing rates in material from the CDZ indicate that creep relaxation during holds is larger than time- and displacement-dependent physicochemical processes that cause frictional healing (Beeler et al., 1994; Niemeijer et al., 2010). This behavior is common in phyllosilicate-rich gouge (Saffer and Marone, 2003; Ikari et al., 2009). In contrast, the positive values of frictional healing for wall rock on both sides of the active CDZ are typical of most quartzofeldspathic rock (Marone, 1998).

Both the near-zero healing rates and velocity strengthening for material from the CDZ are consistent with aseismic creep. Our data also document sharp changes in frictional rate dependence and healing at the edges of the CDZ that parallel the spatial pattern of frictional strength (Figs. 2 and 4). Taken together, our observations predict (1) aseismic creep within the CDZ, and (2) the possibility of earthquake nucleation in material outside and to the northeast of the CDZ, both of which are consistent with observations. Further, extrapolation of our laboratory derived healing rates for wall rock northeast of the CDZ to the observed ~2.7 yr recurrence interval for the SF and LA earthquakes (Nadeau et al., 2004) yields predicted stress drops of ~2–7 MPa in this material (Fig. 2C; Fig. DR4). This is in good agreement with reported stress drops of 1–40 MPa for microearthquakes within 1 km of the fault zone near Parkfield (Allmann and Shearer, 2007), and with a stress drop of 9 MPa for a well-characterized 2003, M_w 2.1, SF event (Imanishi et al., 2004).

SUMMARY

We describe the first friction measurements on intact samples of fault rock from the deep San Andreas fault. Our work provides an integrated view of the frictional strength, slip behavior, and constitutive properties of the SAF at seismogenic depths. The laboratory data offer a coherent explanation for several observations, both long standing and new, including (1) the absolute and relative weakness of the SAF, (2) the extreme localization of fault weakness and the majority of tectonic slip between the North America and Pacific plates to an ~2.6-m-wide fault zone in the CDZ, with a sharp transition to stronger wall rock on either side; (3) fault creep and aseismic slip localized within the CDZ; and (4) repeat-

ing microearthquakes (the LA and SF clusters) with stress drops of 5–10 MPa to the northeast. The pressure-independent shear strength of material from the CDZ above ~60 MPa effective normal stress further suggests that shear strength of the SAF may remain ≤~10 MPa to depths of at least ~5 km.

ACKNOWLEDGMENTS

This research was funded by National Science Foundation grants EAR-054570, EAR-0746192, and OCE-0648331 to Saffer and Marone. We thank Steve Swavely for technical assistance in the laboratory and M. Ikari, A. Neimeijer, M. Scuderi, and C. Collettini for helpful discussions. We also thank B. Holdsworth and an anonymous reviewer for insightful comments that improved this manuscript.

REFERENCES CITED

Allmann, B.P., and Shearer, P.M., 2007, Spatial and temporal stress drop variations in small earthquakes near Parkfield, California: Journal of Geophysical Research, v. 112, B04305, doi:10.1029/2006JB004395.

Beeler, N.M., Tullis, T.E., and Weeks, J.D., 1994, The roles of time and displacement in the evolution effect in rock friction: Geophysical Research Letters, v. 21, p.1987–1990, doi:10.1029/94GL01599.

Carpenter, B.M., Marone, C., and Saffer, D.M., 2009, Frictional behavior of materials in the 3D SAFOD volume: Geophysical Research Letters, v. 36, L05302, doi:10.1029/2008GL036660.

Carpenter, B.M., Marone, C., and Saffer, D.M., 2011, Weakness of the San Andreas Fault revealed by samples from the active fault zone: Nature Geoscience, v. 4, p. 251–254, doi:10.1038/ngeo1089.

Collettini, C., Niemeijer, A., Viti, C., and Marone, C., 2009, Fault zone fabric and fault weakness: Nature, v. 462, p. 907–910, doi:10.1038/nature08585.

Di Toro, G., Han, R., Hirose, T., De Paola, N., Nielsen, S., Mizoguchi, K., Ferri, F., Cocco, M., and Shimamoto, T., 2011, Fault lubrication during earthquakes: Nature, v. 471, p. 494–498, doi:10.1038/nature09838.

Fulton, P.M., and Saffer, D.M., 2009, Potential role of mantle-derived fluids in weakening the San Andreas Fault: Journal of Geophysical Research, v. 114, B07408, doi:10.1029/2008JB006087.

Goldsby, D.L., and Tullis, T.E., 2002, Low friction strength of quartz rocks at subseismic slip rates: Geophysical Research Letters, v. 29, 1844, doi:10.1029/2002GL015240.

Gratier, J.-P., Richard, J., Renard, F., Mittempergher, S., Doan, M.-L., Di Toro, G., Hadizadeh, J., and Boullier, A.M., 2011, Aseismic sliding of active faults by pressure solution creep: Evidence from the San Andreas Fault Observatory at Depth: Geology, v. 39, p. 1131–1134, doi:10.1130/G32073.1.

Hickman, S., and Zoback, M., 2004, Stress orientations and magnitudes in the SAFOD pilot hole: Geophysical Research Letters, v. 31, L15S12, doi:10.1029/2004GL020043.

Hickman, S., Zoback, M., and Ellsworth, W., 2004, Introduction to special section: Preparing for the San Andreas Fault Observatory at Depth: Geophysical Research Letters, v. 31, L12S01, doi:10.1029/2004GL020688.

Holdsworth, R.E., van Diggelen, E.W.E., Spiers, C.J., de Bresser, J.H.P., Walker, R.J., and Bowen, L., 2011, Fault rocks from the SAFOD core samples: Implications for weakening at shallow depths along the San Andreas Fault, California: Journal of Structural Geology, v. 33, p. 132–144, doi:10.1016/j.jsg.2010.11.010.

Ikari, M.J., Saffer, D.M., and Marone, C., 2009, Frictional and hydrologic properties of clay-rich fault gouge: Journal of Geophysical Research, v. 114, B05409, doi:10.1029/2008JB006089.

Imanishi, K., Ellsworth, W.L., and Prejean, S.G., 2004, Earthquake source parameters determined by the SAFOD Pilot Hole seismic array: Geophysical Research Letters, v. 31, L12S09, doi:10.1029/2004GL019420.

Inoue, A., and Utada, M., 1991, Smectite-to-chlorite transformation in thermally metamorphosed volcaniclastic rocks in the Kamikita area, northern Hinshu, Japan: American Mineralogist, v. 79, p. 628–640.

Kinoshita, M., Tobin, H., Ashi, J., Kimura, G., Lallemant, S., Screaton, E.J., Curewitz, D., Masago, H., and Moe, K.T., and the Expedition 314/315/316 Scientists, 2009, IODP Proceedings, 314/315/316: Washington, D.C., Integrated Ocean Drilling Program Management International, Inc., doi:10.2204/iodp.proc.314315316.134.2009.

Lachenbruch, A.H., and Sass, J.H., 1980, Heat flow and energetics of the San Andreas fault zone: Journal of Geophysical Research, v. 85, p. 6185–6222, doi:10.1029/JB085iB11p06185.

Lockner, D.A., Morrow, C., Moore, D., and Hickman, S., 2011, Low strength of deep San Andreas fault gouge from SAFOD core: Nature, v. 472, p. 82–85, doi:10.1038/nature09927.

Ma, K.F., and 12 others, 2006, Slip zone and energetics of a large earthquake from the Taiwan Chelungpu-fault Drilling Project: Nature, v. 444, p. 473–476, doi:10.1038/nature05253.

Marone, C., 1998, Laboratory-derived friction laws and their application to seismic faulting: Annual Review of Earth and Planetary Sciences, v. 26, p. 643–696, doi:10.1146/annurev.earth.26.1.643.

Melosh, H.J., 1996, Dynamical weakening of faults by acoustic fluidization: Nature, v. 379, p. 601–606, doi:10.1038/379601a0.

Nadeau, R.M., Michelini, A., Uhrhammer, R.A., Dolenc, D., and McEvilly, T.E., 2004, Detailed kinematics, structure and recurrence of micro-seismicity in the SAFOD target region: Geophysical Research Letters, v. 31, L12S08, doi:10.1029/2003GL019409.

Niemeijer, A., Marone, C., and Elsworth, D., 2010, Frictional strength and strain weakening in simulated fault gouge: Competition between geometrical weakening and chemical strengthening: Journal of Geophysical Research, v. 115, B10207, doi:10.1029/2009JB000838.

Rice, J.R., 1992, Fault stress states, pore pressure distributions, and the weakness of the San Andreas Fault, *in* Evan, B., and Wong, T.-F., eds., Fault mechanics and transport properties of rocks: San Diego, California, Academic Press, Ltd., p. 475–503.

Saffer, D.M., and Marone, C., 2003, Comparison of smectite and illite frictional properties: Application to the updip limit of the seismogenic zone along subduction megathrusts: Earth and Planetary Science Letters, v. 215, p. 219–235, doi:10.1016/S0012-821X(03)00424-2.

Schleicher, A.M., van der Pluijm, B.A., and Warr, L.N., 2010, Nanocoatings of clay and creep of the San Andreas fault at Parkfield, California: Geology, v. 38, p. 667–670, doi:10.1130/G31091.1.

Tembe, S., Lockner, D.A., Solum, J.G., Morrow, C.A., Wong, T., and Moore, D.E., 2006, Frictional strength of cuttings and core from SAFOD drillhole phases 1 and 2: Geophysical Research Letters, v. 33, L23307, doi:10.1029/2006GL027626.

Thayer, M.R., and Arrowsmith, J.R., 2005, Fault zone structure of Middle Mountain, central California: Eos (Transactions, American Geophysical Union), v. 86, abs. T21A–0458.

Thordsen, J.J., Evans, W.C., Kharaka, Y.K., Kennedy, B.M., and van Soest, M., 2005, Chemical and isotopic composition of water and gases from the SAFOD wells: Implications to the dynamics of the San Andreas fault at Parkfield, California: Eos (Transactions, American Geophysical Union), v. 86, abs. T23E–08.

Thurber, C.H., Roecker, S.W., Zhang, H., Bennington, N.L., and Peterson, D., 2010, Crustal structure and seismicity around SAFOD: A ten-year perspective: Eos (Transactions, American Geophysical Union), v. 91, abs. T52B–01.

Zoback, M., Hickman, S., Ellsworth, W., and SAFOD Science Team, 2011, Scientific drilling into the San Andreas Fault zone—An overview of SAFOD's first five years: Scientific Drilling, no. 11, p. 14–28, doi:10.2204/iodp.sd.11.02.2011.

Zoback, M.D., and 12 others, 1987, New evidence on the state of stress on the San Andreas fault system: Science, v. 238, p. 1105–1111, doi:10.1126/science.238.4830.1105.

Manuscript received 8 November 2011
Revised manuscript received 9 March 2012
Manuscript accepted 16 March 2012

Printed in USA